



Vietnam Academy of Science and Technology

Vietnam Journal of Marine Science and Technology

journal homepage: vjs.ac.vn/index.php/jmst



Effects of tides, waves, and sea dikes on storm surge-induced coastal flooding in the Thanh Hoa region

Pham Van Tien¹, Nguyen Ba Thuy^{2*}, Nguyen Kim Cuong³, Vu Hai Dang⁴, Bui Manh Ha²,
Nguyen Phuong Anh², Sooyoul Kim⁵, Lars Robert Hole⁶

¹*Institute of Meteorology, Hydrology and Climate Change, Hanoi, Vietnam*

²*National Center for Hydro-Meteorological Forecasting, Hanoi, Vietnam*

³*University of Science, Vietnam National University, Hanoi, Vietnam*

⁴*Institute of Earth Sciences, VAST, Vietnam*

⁵*Center for Water Cycle, Marine Environment and Disaster Management, Kumamoto University, Japan*

⁶*Division of Oceanography and Maritime Meteorology, Norwegian Meteorological Institute, Bergen, Norway*

Received: 25 June 2025; Accepted: 6 September 2025

ABSTRACT

In this study, the impacts of tides, ocean waves, and sea dikes on coastal flooding in Thanh Hoa Province caused by storm surge in combination with tides were evaluated using simulated flooding results for Typhoon Doksuri (September 2017). The simulations were conducted with the SuWAT numerical model, in which tide, wave, and storm surge processes were integrated. The SuWAT model was developed using a moving-boundary algorithm to simulate flooding driven by tidal variations and storm surges. The results indicate that, for Typhoon Doksuri (September 2017), when the typhoon landfall occurred during the highest tidal phase, the total inundated area in the study region increased by approximately 21.9% compared with the landfall time during the lowest tidal phase. When wave-induced effects were included in the model, the inundated area increased by about 7.2% relative to the case without wave influence. In the scenario without sea dikes along the Thanh Hoa coast, the total flooded area increased by approximately 69.0% compared to the case with real existing dikes. These findings provide valuable insights for coastal zone planning and for improving flood forecasting and early warning systems related to tidal and storm surge-induced flooding in the study area.

Keywords: Typhoon, tide, ocean waves, storm surge, coastal flooding, integrated SuWAT model, Doksuri, moving boundary, Thanh Hoa.

*Corresponding author at: National Centre for Hydro-Meteorological Forecasting, Vietnam Meteorology Hydrology Administration, Floor 12, No 24, Huynh Thuc Khang, Hanoi, Vietnam. *E-mail addresses:* thuybanguyen@gmail.com

Introduction

Storm surge is one of the most hazardous marine disasters, leading to coastal flooding, shoreline erosion, and saltwater intrusion caused by elevated sea levels accompanied by large waves. Under the impacts of climate change, the occurrence of intense and even super typhoons with unpredictable behaviors is expected to increase, posing greater risks to the mainland of Vietnam. Historically, numerous typhoons in Vietnam were produced severe storm surges and large waves that overtopped and breached sea dikes, resulting in extensive coastal flooding. Since 2005, several typhoons have made landfall during high-tide periods, with storm surge heights ranging from 1 to 2 meters, causing dike failures and severe inundation. Examples include Typhoon Washi (2005) in Hai Phong, Typhoon Damrey (2005) in Nam Dinh, Typhoons Xangsane (2006) and Ketsana (2009) in Hue and Da Nang, Typhoon

Kalmaegi (2014) in Quang Ninh, Typhoon Doksuri (2017) in Nghe An–Ha Tinh, and Typhoon Vamco (2020) in Quang Binh–Quang Tri [1–5]. Typhoon Damrey (September 2005), with wind speeds of 10–11 on the Beaufort scale, directly landfalled along the Nam Dinh coast during a spring tide, generating strong storm surge and large waves that breached sea dikes and inundated wide coastal areas in Nam Dinh, Ninh Binh, and Thanh Hoa [1]. Typhoon Doksuri (September 2017) struck the Quang Binh–Ha Tinh coast at the time of high tide in northern Vietnam, causing widespread overtopping of sea dikes from Hai Phong to Ha Tinh and flooding in low-lying coastal zones (Fig. 1) [6]. Due to the devastating impacts of such events, extensive studies on typhoons and storm surges have been conducted using various approaches to improve forecasting and early warning systems, as well as to support coastal planning and the design of marine and coastal infrastructure.



Figure 1. Coastal flooding caused by storm surge and waves along the Thanh Hoa coast during Typhoon Doksuri in September 2017: (a) Sam Son coast; (b) Hau Loc sea dike [7, 10]

Besides to topography, coastal protection structures, and river discharge from upstream areas, the extent of coastal flooding induced by typhoons depends on the total coastal water level, which consists of tidal level, wind- and pressure-induced surge, and wave setup. These components are described and illustrated in Figures 2a–b as follows:

$$H_t = H_{tide} + H_{storm\ surge} \quad (1)$$

in which: H_t : total water level; H_{tide} : tidal level; $H_{storm\ surge}$: storm surges.

$$H_{storm\ surge} = H_{wind+pressure} + H_{wave} \quad (2)$$

where: $H_{wind+pressure}$: surges induced by wind and pressure; H_{wave} : wave setup.

In this context, wave setup refers to the increase in mean water level caused by wave

radiation stress and wave-induced surface stress. The component generated by radiation stress results from the conversion of wave kinetic energy into the potential energy of the water column.

In Vietnam, several studies on storm surge have been conducted using various approaches to support forecasting, early warning, planning and designing of marine and coastal structures. Examples include works by Chien et al. (2014) [2], Thuy et al. (2017) [3], Thuy et al. (2020) [4], and Tien et al. (2025) [5]. However, due to computational limitations, most existing studies have mainly focused on assessing and developing technologies for predicting and warning storm surge heights at the shoreline. Research specifically addressing coastal flooding induced by storm surge remains limited. Several notable studies on coastal inundation caused by storm surge include: Lien (2010), who evaluated coastal

risk in Thua Thien-Hue Province under sea-level rise scenarios and developed a decision-support tool for inundation scenarios corresponding to return periods of 1, 2, 5, 10, and 20% [8]; the General Department of Disaster Prevention and Control, Ministry of Agriculture and Rural Development (2016), which produced coastal inundation hazard maps for strong and super typhoon scenarios making landfall along the Vietnamese coast—although this project focused only on specific storm landfall scenarios with intensities ranging from Category 12 to 16 and selected tidal phases [9]; and more recently, Tien et al. (2023) simulated coastal inundation risks in Thanh Hoa Province under several typhoon landfall scenarios using the integrated numerical model SuWAT. However, in that study, the simulations were performed at mean sea level conditions without considering tidal fluctuations during storm impact [10].

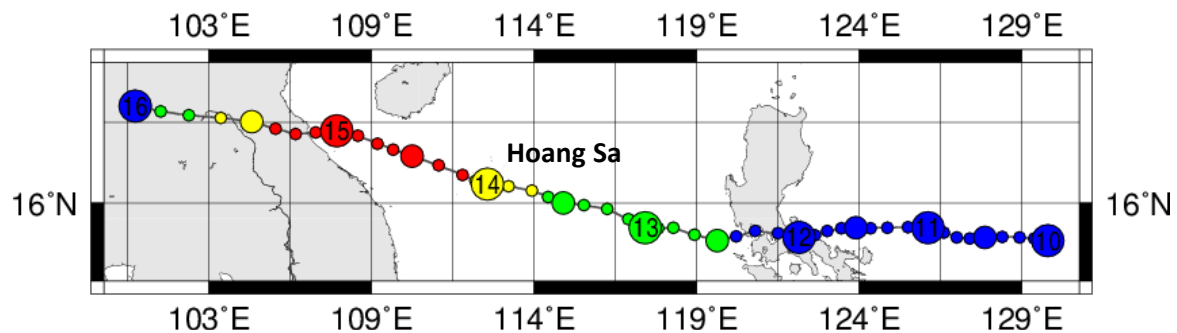


Figure 2. Track of Typhoon Doksuri (September 2017) making landfall along the Quang Binh–Ha Tinh coast

The climate change, characterized by the rising trend of mean sea level and increasingly complex patterns of storms and floods, is heightening the risk of inundation in low-lying coastal areas. Many countries around the world are facing this challenge. To assess current and future coastal flood risks, Indonesian researchers have developed a GIS-based system integrated with numerical model outputs to generate flood maps for coastal flood events (Lee et al., 2020) [11]. The modeling components in this system include the hydrodynamic model DELFT-3D for predicting tides and wind-induced storm surge, and the WAVEWATCH III model for wave forecasting. In Bangladesh, to evaluate vulnerability to major storms and sea-level rise projected for the year

2050, Dasgupta et al. (2010) employed an integrated approach combining climate change information, hydrodynamic modeling, and geographic data layers [12]. In the Caribbean region, coastal flooding and storm tides frequently occur due to tropical cyclones (hurricanes), which generate storm surge, large waves, heavy rainfall, and riverine flooding. To improve forecasting and early warning, the region has applied the SLOSH model and performed ensemble simulations covering numerous possible scenarios of hurricane tracks, intensities, and forward speeds using a supercomputing platform. Instead of executing a single high-resolution real-time model run, the flood forecasting system accesses precomputed results from hundreds of possible scenarios

representing variations in tropical cyclone characteristics and wave conditions to provide rapid inundation forecasts [13]. For coastal flood warnings, scientists have adopted various approaches, with numerical modeling being the preferred method, as it allows for the combined assessment of all contributing factors—storm surge generation mechanisms and the impacts of global sea-level rise [14].

With the second approach, studies have focused on developing and improving numerical models for forecasting and evaluating the influence of various factors, such as wind, atmospheric pressure, waves, coastal and estuarine topography, on flooding in specific regions. Over time, coastal flood forecasting models for storm surge have become increasingly sophisticated. Two- and three-dimensional, as well as fully coupled, models have been developed to incorporate multiple interacting processes, while grid resolution has improved with advances in computational capacity.

In addition to the effects of wind and pressure forcing, the influence of waves on storm surge and coastal inundation has been examined in many forecasting systems through the integration of storm surge and wave models (e.g., Wolf, 2008; Chen et al., 2010; Li et al., 2013; Yin and Yu, 2016; Wu et al., 2018; Murty et al., 2020) [15–20]. Wolf (2008) tested an integrated tide–wave–surge model for the historic flooding event associated with Cyclone Nargis, which made landfall in Myanmar in May 2008, and demonstrated that wave setup in shallow coastal waters significantly contributed to the overall extent of inundation [15]. Murty et al. (2020) assessed the impact of wave radiation stress on storm surge and coastal flooding along the west coast of India by comparing results from the ADCIRC model with those from the coupled ADCIRC + SWAN system. The coupled model produced surge and inundation levels 20–30% higher than those of the uncoupled model. The authors therefore recommended using coupled hydrodynamic-wave models for forecasting storm surge and coastal flooding [20].

In this study, the integrated SuWAT model, which combines tides, ocean waves, and storm

surge processes, was enhanced with a moving-boundary algorithm to simulate coastal flooding induced by storm surge [1–6, 10, 21–23]. The effects of tides, waves, and sea dikes on coastal inundation in Thanh Hoa Province were numerically simulated and analyzed.

Study area, datasets, and methodology

Study area

In this study, the simulation domain for coastal flooding covers the coastal zone from Hau Loc to Sam Son in Thanh Hoa Province. This region has experienced extensive inundation caused by storm surges combined with high tides during several typhoon events affecting the area, such as Wukong (September 2000), Damrey (September 2005), Talas (July 2017), and Doksuri (September 2017). Another reason for selecting this coastal stretch is the availability of recently updated datasets on topography (both subaqueous and terrestrial elevations) and coastal protection structures (including dikes, revetments, and transportation embankments—collectively referred to as sea dikes). These datasets, which are critical factors influencing storm surge and coastal inundation, were updated as part of a national-level scientific project coded ĐTDL.CN-46/22, conducted during October–November 2023.

Datasets

In this study, bathymetric data for the East Vietnam Sea were obtained from the General Bathymetric Chart of the Oceans (GEBCO), updated in 2024, with a spatial resolution of 15 arc-seconds (https://www.gebco.net/data_and_products/gridded_bathymetry_data/). Topographic data for the coastal areas of Thanh Hoa Province and adjacent regions were collected from the Department of Surveying, Mapping, and Geographic Information of Vietnam, at map scales ranging from 1:10,000 to 1:25,000.

Typhoon Doksuri (September 2017), which made landfall along the Ha Tinh–Quang Binh coast (track shown in Fig. 2), was selected for

simulation. The storm struck during a period of high spring tide along the northern Vietnam coast, generating large waves and significant storm surge that caused widespread overtopping of sea dikes from Hai Phong to Nghe An [6]. Observations at the Hon Dau and Hon Ngu hydrographic stations recorded maximum storm surges of 0.78 m and 0.98 m, respectively [6].

Reanalysis wind and atmospheric pressure data with a spatial resolution of 0.25° were obtained from the European Centre for Medium-Range Weather Forecasts (ECMWF, ERA5 dataset) and interpolated onto the outermost computational grid domain (D1 - Fig. 3a) for the coastal flooding simulations associated with Typhoon Doksuri (September 2017) [24].

Study methodology

In this study, the integrated Surge–Wave–Tide model (SuWAT) was employed to simulate tides, ocean waves, and storm surges. This model has been utilized in several previous studies [1–6, 21–23] and was applied here to reproduce coastal flooding induced by the combined effects of tides and storm surge. The model has been further developed to include a moving-boundary algorithm for simulating inundation processes [10]. Figure 3 illustrates the moving-boundary algorithm of the SuWAT model along the x-direction (longitude), where the variable “land” defines the wet–dry status

of a grid cell. In the model, a grid point is considered flooded (wet) when $\text{land} = 0$ and dry (unflooded) when $\text{land} = 1$. During each time step, the water level at each grid point ($Z(i,j)$) is compared with the local elevation ($H(i,j)$) to determine whether water overtops the dry surface, allowing flow into or out of the cell depending on the relative magnitudes of water level and topography. The same procedure is applied in the y-direction. Further details of the model are described in Tien et al. (2023) [10]. In previous studies, the SuWAT model was validated for water level, tide, storm surge, and wave simulations using Typhoon Doksuri (September 2017) as a case study [6, 10]. The open boundary of the outermost domain (D1) included 16 primary tidal constituents: M_2 , S_2 , K_1 , O_1 , N_2 , P_1 , K_2 , Q_1 , M_1 , J_1 , OO_1 , $2N_2$, Mu_2 , Nu_2 , L_2 , and T_2 . Wave radiation stress was calculated using the formulation of Janssen (1991), as introduced by Kim et al. (2010) [23] and later applied by Tien et al. (2025) [6]. The nested-grid system was implemented such that, at each time step, the simulated values of tide, surge, and wave parameters at the boundary of a coarser grid were used as input for the next finer grid. The simulation time step was 4 seconds for the tide–surge model and 900 seconds for the wave model. The optimal sea-surface roughness coefficient was set to 0.025, while the roughness coefficient over flooded land areas was assigned an average value of 0.05, corresponding to typical coastal terrain conditions.

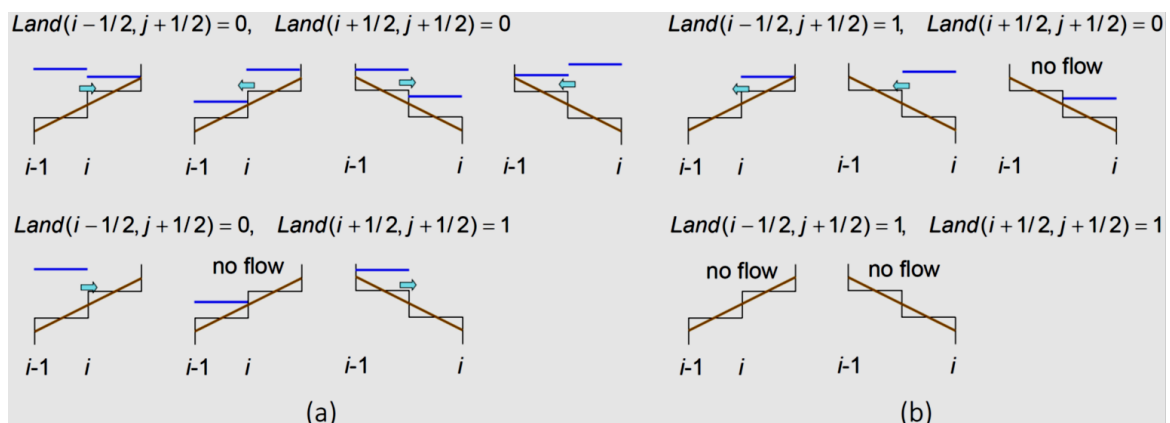


Figure 3. Description of the moving-boundary algorithm in the SuWAT model

To simulate coastal flooding induced by storm surges in the study area, the SuWAT model was configured using a square, six-level nested grid system. Among these, the innermost domain (D6) covers the coastal zone from Hau Loc to Sam Son, incorporating the most recently updated

topographic and sea dike data obtained from the national-level research project ĐTDL.CN-46/22. All topographic data were referenced to the national vertical datum. Details of the computational domains and grid resolutions are presented in Table 1 and Figure 4.

Table 1. Computational domains and grid resolutions of the model

Domain	Longitude (°E)	Latitude (°N)	Resolution (°)	No. of grid points along the longitudinal direction	No. of grid points along the latitudinal direction
D1	105.000–120.000	8.000–22.000	0.045	371	345
D2	105.000–112.550	14.000–22.000	0.015	556	556
D3	105.000–108.500	17.500–21.500	0.005	778	889
D4	105.748–106.500	19.200–20.225	0.003	279	378
D5	105.748–106.263	19.450–20.073	0.001	778	889
D6	105.748–106.053	19.688–19.995	0.000539	567	571

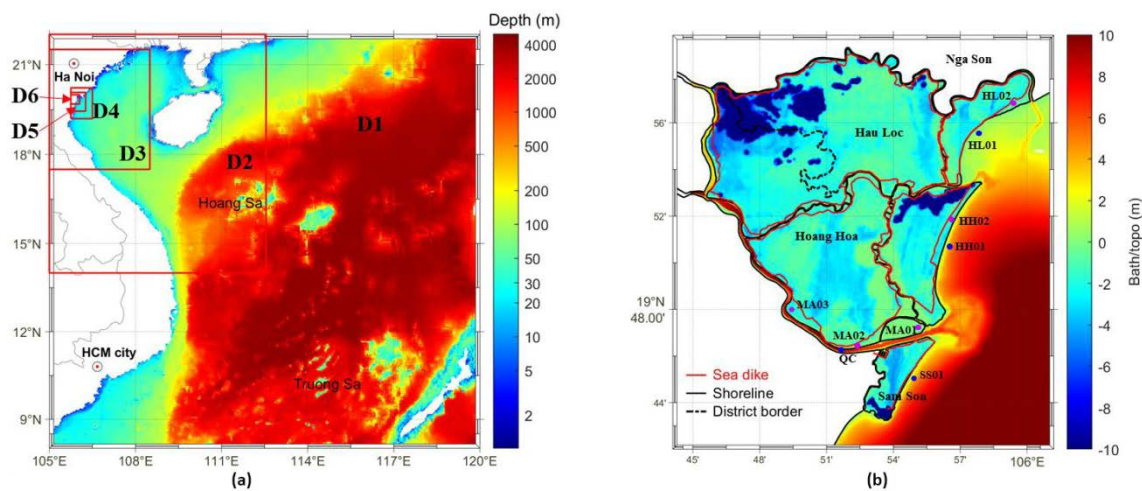


Figure 4. (a) Layout of the six nested computational grids of the model; (b) detailed bathymetry of the innermost domain (D6) covering the Hau Loc–Sam Son coastal area in Thanh Hoa Province, and locations of data extraction points

Results and discussion

Evolution of storm surge-induced coastal flooding in Thanh Hoa Province

In this study, a location was considered inundated if its elevation was higher than the mean sea level but was temporarily overtopped when the combined water level exceeded the ground elevation. Temporal variations in tides, combined with storm surges, caused the sea

level to rise above the land surface at certain times, resulting in flooding. Figure 5 presents the simulated evolution of the total water level (tide + storm surge) during Typhoon Doksuri (September 2017) when the storm made landfall during a high-tide phase, at four representative times: at 23:00 (GMT), 14 September 2017 - approximately nine hours before landfall (Fig. 5a). At this time, the coastal water level was near the mean tidal level, with no significant rise or fall due to wind

or wave effects. At 03:00, 15 September 2017, the time of maximum water level, the storm surge coincided with the high-tide peak (Fig. 5b). At this stage, many inland areas had become inundated. At 15:00 on 15 September 2017, as the water level began to recede, most

previously flooded areas were no longer submerged, or the inundation depth had considerably decreased (Fig. 5c). At 19:00 on 15 September 2017, the lowest water level was reached, indicating that inundation had completely subsided across the region (Fig. 5d).

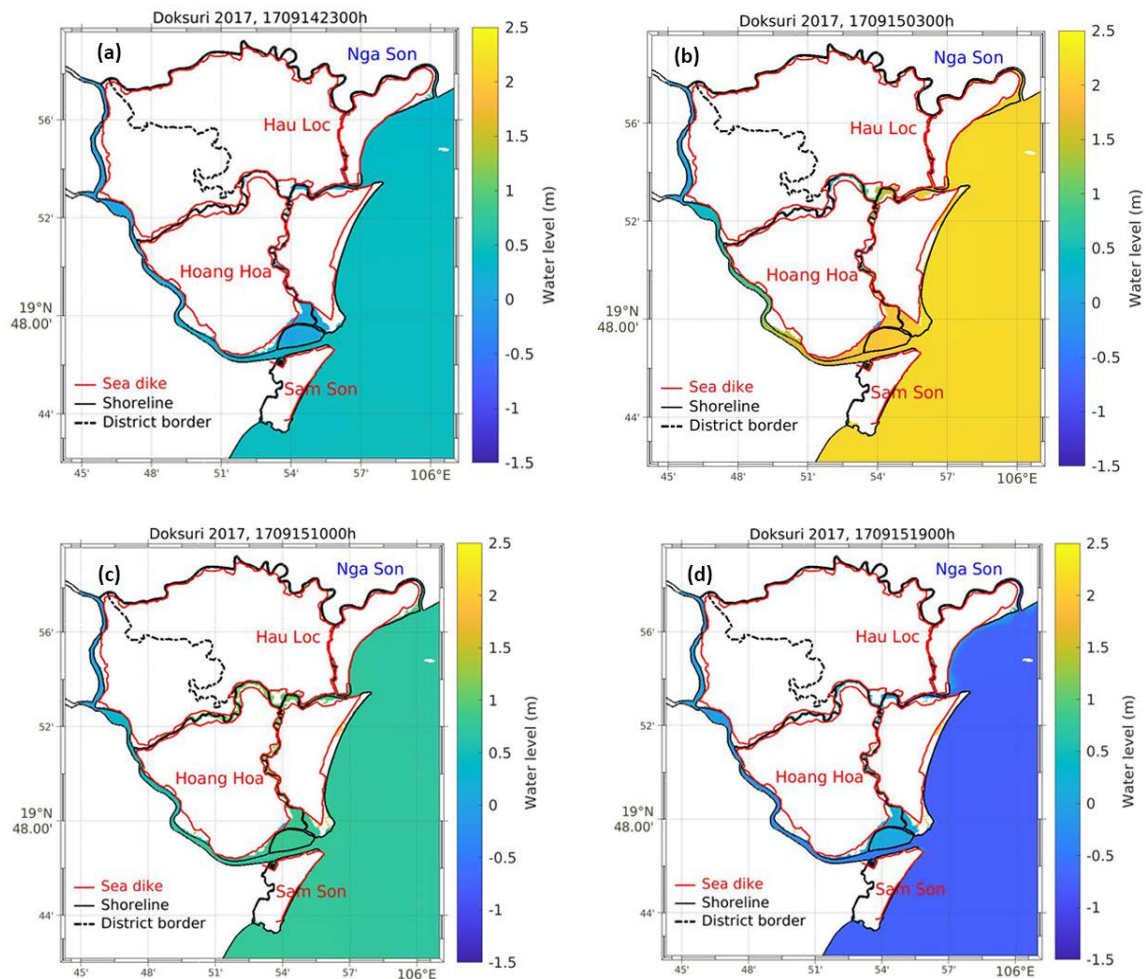


Figure 5. Spatial distribution of water level variations at different times: (a) Mean tidal level before wind influence, (b) Maximum combined water level (tide + storm surge), (c) Receding water level, and (d) Lowest water level

Influence of tidal phase on coastal flooding in Thanh Hoa Province

To evaluate the influence of tidal phase on coastal flooding in Thanh Hoa Province, this study simulated the storm surge and flooding caused by Typhoon Doksuri (September 2017) under three different tidal phases—high tide,

mean tide, and low tide—as illustrated in Figure 6. Tien et al. (2025) previously investigated the effect of tidal phase on storm surge height during Typhoon Doksuri (2017) along the northern coast of Vietnam. Their results showed that the highest storm surge occurred when the typhoon made landfall during the low-tide phase, while the smaller

surge was associated with landfall during high tide [6]. However, that study did not assess the total water level (i.e., the combined effect of tide and storm surge) or the resulting inundation extent for these three tidal phase scenarios. In the present study, the model simulations excluded wave effects to isolate the impact of tidal phase. Figures 7a–c present the simulated time series of total water levels at three representative locations: Hau Loc (Fig. 6a), Sam Son (Fig. 7b), and Quang Chau station (Fig. 4b, located about 4 km inland along the Lam River) (Fig. 7c). Each panel compares results for tidal forcing alone (no storm) with the three tidal-phase scenarios.

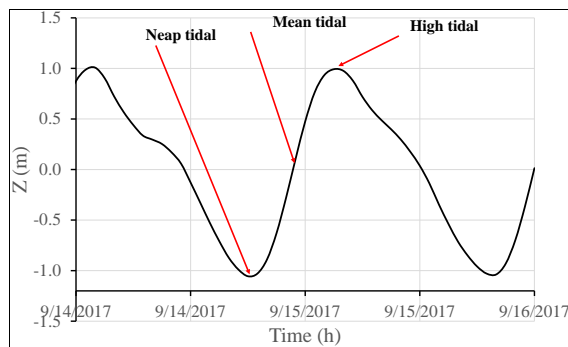


Figure 6. Illustration of the landfall timing of Typhoon Doksuri (September 2017) corresponding to three tidal phases in the coastal flooding simulation for the Thanh Hoa coastal area

The results indicate that at all three locations, the highest total water levels occur when the typhoon coincides with the high-tide phase, followed by the mean-tide phase. The low-tide scenario still produces higher water levels than the pure-tide case due to the contribution from storm surge. At the inland Quang Chau station, total water levels are lower, and the timing of peak water level is delayed relative to the coastal sites (Hau Loc and Sam Son). These findings are consistent with Tien et al. (2025) [6]: although storm surge height alone is greater when the typhoon strikes at low tide, the tidal amplitude in this region is larger than the surge height. Consequently, the total water level remains highest when the storm coincides with high tide.

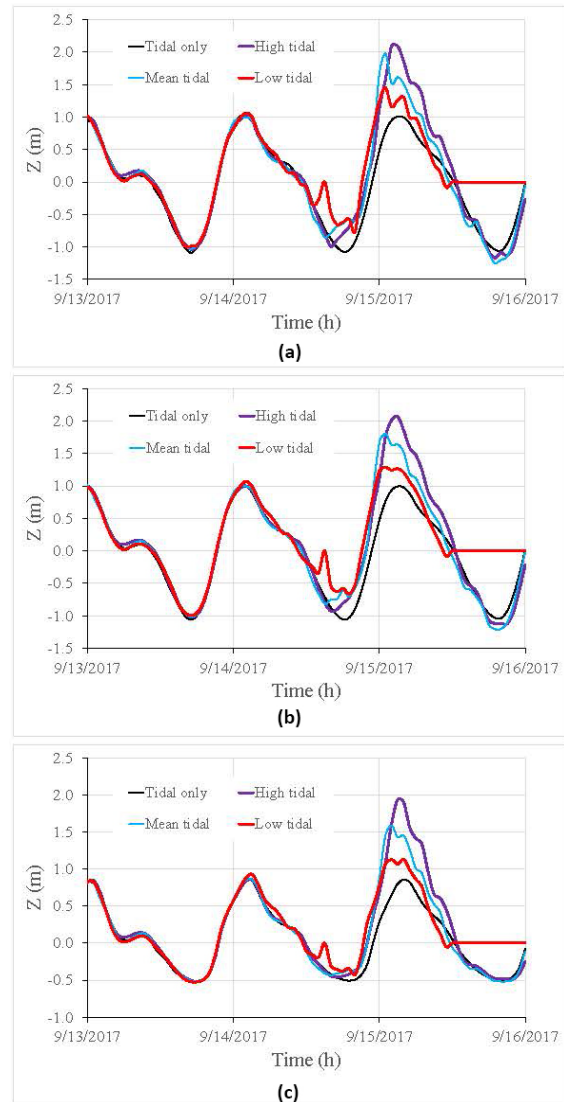


Figure 7. Variations of total water level during the typhoon under different simulation scenarios at locations: (a) Hau Loc coastal area (HL01), (b) Sam Son coastal area (SS01), and (c) Quang Chau station (QC)

The extent and depth of coastal flooding depend directly on the total water level; therefore, when a typhoon makes landfall during different tidal phases, the resulting inundation extent also varies. The spatial distribution of maximum flood depth of four simulation cases - (1) tide only (at high tide), (2) typhoon landfall during low tide, (3) mean tide, and (4) high tide - is shown in Figure 8, while

the total inundated area for each case is summarized in Figure 8. Because a coastal dike system protects the study area, the flooded zones are mainly concentrated in low-lying areas outside the sea dike of Hau Loc District and around the Ma and Leng river basins. The results reveal clear differences in both the extent and depth of flooding (Fig. 8) and in the total inundated area (Fig. 9) among the scenarios. When the typhoon coincides with high tide, the total inundated area reaches its maximum of about 28.3 km². For the mean-tide and low-tide cases, the inundated areas are approximately 27.2 and 22.1 km²,

corresponding to reductions of 3.9 and 21.9%, respectively, compared with the high-tide case. In contrast, under the tide-only condition (no storm), the inundated area is about 21.5 km². Although the inundation area during low tide remains slightly larger than that under the tide-only case, the difference is relatively small. Overall, the simulation results for Typhoon Doksuri (September 2017) indicate that the highest coastal flooding risk in Thanh Hoa Province occurs when the typhoon makes landfall during high tide. In contrast, flooding is significantly reduced when the storm coincides with low tide.

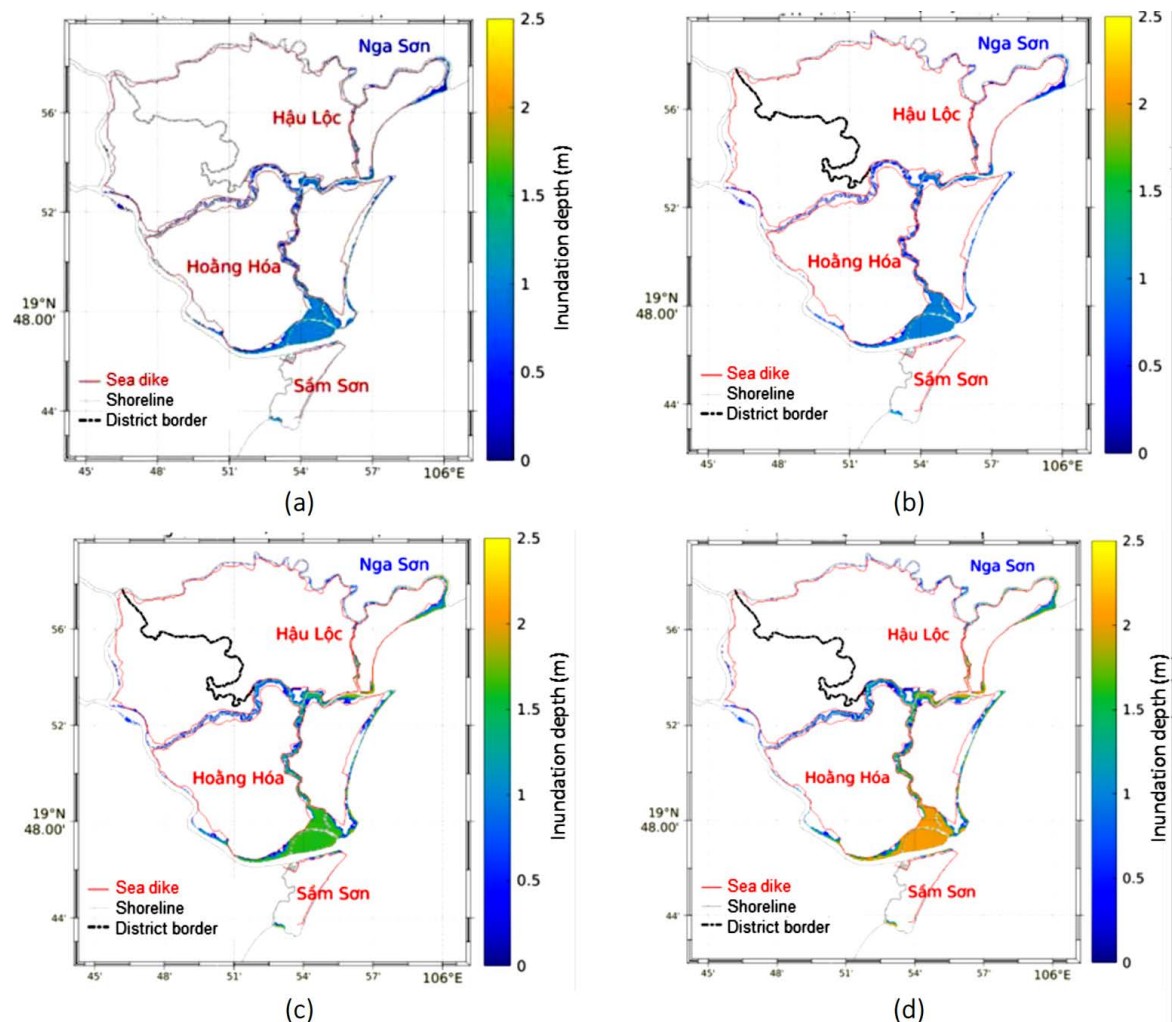


Figure 8. Spatial distribution of maximum inundation depth under different simulation scenarios: (a) tidal peak only, (b) typhoon landfall at low-tide phase, (c) typhoon landfall at mean-tide phase, and (d) typhoon landfall at high-tide phase

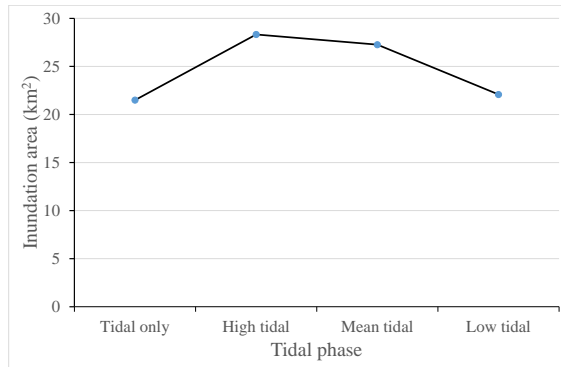


Figure 9. Total inundated area under different simulation scenarios

Effect of ocean waves on coastal flooding in Thanh Hoa Province

The influence of waves on coastal flooding is defined as the difference in the extent and depth of inundation between simulations with and without the inclusion of wave effects—that is, between the simulation considering only wind and atmospheric pressure forcing, and the simulation considering the combined effects of wind, pressure, and waves during the storm. In the study by Tien et al. (2025), the influence of waves on storm surge during Typhoon Doksuri (September 2017) was estimated to contribute approximately 10–15% of the total surge height at the Hon Dau and Hon Ngu stations [6]. However, that study did

not assess the impact of waves on coastal inundation in the study area. To evaluate the influence of ocean waves on coastal flooding caused by the storm, the simulation scenario of Typhoon Doksuri (September 2017) making landfall during the high-tide phase was selected. The spatial distributions of maximum inundation depth for simulations with and without wave effects are shown in Figure 10, where Figure 10a represents the scenario without wave effects and Figure 10b represents the scenario with wave effects included. The notable differences between the two scenarios are evident along the northern bank of the Ma River basin, where the simulation incorporating wave effects reveals a wider inundated area and deeper inundation depths at the corresponding locations. The statistical results of the inundated area by depth range are presented in Table 2, indicating that the scenario including wave effects results in a total inundated area of approximately 30.5 km², which is about 7.2% larger than the simulation excluding wave effects. The data in Table 2 also show that the largest proportion of flooded area corresponds to inundation depths between 1.5 and 2.0 m. When wave effects are included, approximately 2.7 km² of land experiences inundation depths ranging from 2.0 to 2.5 m. In contrast, the simulation without waves yields a maximum inundation depth of only 2.0 m.

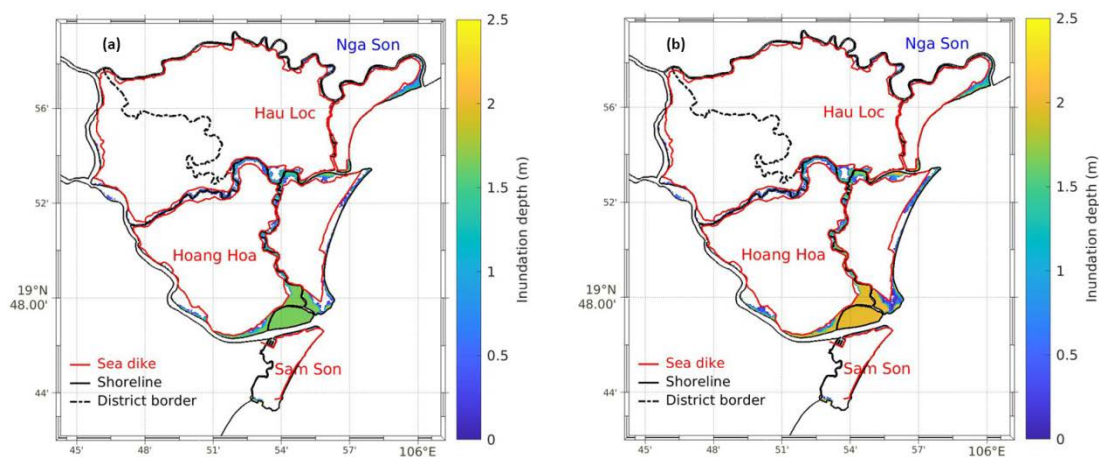


Figure 10. Distribution of maximum inundation depth for simulations (a) without and (b) with consideration of wave effects

Table 2. Statistics of inundated area by depth range for simulation cases with and without consideration of wave effects

Inundation depth range (m)	Inundated area (km ²)	
	Scenario without wave consideration	Scenario with wave consideration
< 0.5	4.9	5.3
0.5–(> 1.0)	5.2	5.4
1.0–(> 1.5)	6.7	4.7
1.5–(> 2.0)	11.3	12.5
2.0–(> 2.5)	0.0	2.7
2.5–(> 3.0)	0.0	0.0
Total	28.3	30.5

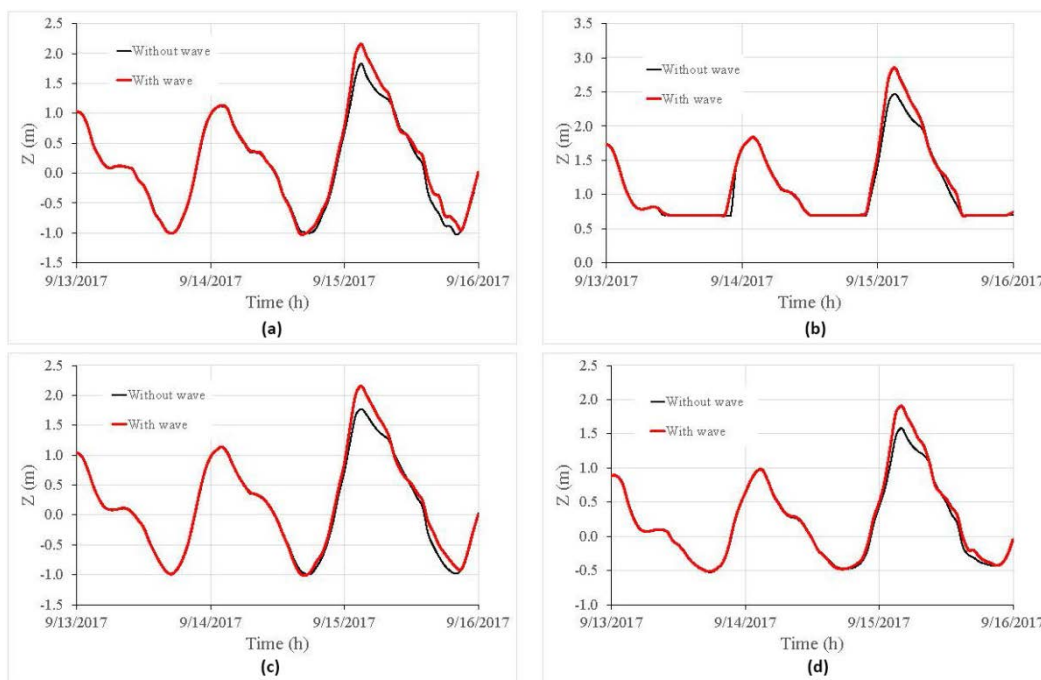


Figure 11. Variations of total water level during the storm for simulation scenarios with and without consideration of wave effects at locations: (a) HL01, (b) HL02, (c) SS01, and (d) QC

To further clarify the role of ocean waves in coastal flooding during storm landfall, the simulated time series of water level variations at four locations (Figure 4b) are presented in Figure 11. Among these, location HL02 is situated on land, outside the Hau Loc sea dike, with an elevation of 0.7 m above mean sea level. It can be observed that, compared with the simulation without wave effects, the simulation including wave effects yields higher total water levels at all locations. The maximum difference in total water level between the two scenarios occurs at the onshore point HL02,

with an increase of 0.39 m, which is greater than the 0.32 m difference observed at the offshore point HL01. This result indicates that the wave-induced surge effect becomes more significant in shallower coastal zones. Although no direct observational data are available to validate the inundation simulation results, the modeled flooding patterns for the Thanh Hoa coastal region during Typhoon Doksuri (September 2017) show reasonable agreement with qualitative information obtained from the project “Research on the development of a model system and

technological procedure for forecasting coastal inundation caused by storm surge and waves”, which collected reports from the Thanh Hoa Department of Agriculture and Environment and local residents in July 2023.

Influence of sea dikes on coastal flooding in Thanh Hoa Province

To evaluate the influence of sea dikes in Thanh Hoa on coastal flooding due to typhoon, simulations were conducted using the SuWAT model to reproduce storm surge-induced inundation combined with tides for the case of Typhoon Doksuri (September 2017) making landfall during the high-tide phase, under the assumption that no sea dikes existed along the Thanh Hoa coastline. The simulation scenario considering wave effects was selected to

represent the worst-case flooding condition. The simulated inundation extent without dikes (Fig. 12b) was compared with the scenario including sea dikes (Fig. 12a). The results show that, in the absence of sea dikes, the inundated area expanded significantly, with a total flooded area of approximately 98.3 km², representing a 69.0% increase. Regarding inundation depth, the no-dike scenario exhibited a larger proportion of shallowly flooded areas compared with the case including sea dikes, with most inundation depths being less than 0.5 m (Fig. 13). This is primarily because, in the presence of sea dikes, water accumulation was restricted within enclosed, low-lying zones, resulting in higher local inundation depths. In contrast, in the no-dike condition, water could flow more freely in and out, leading to a quicker rise and fall of water levels.

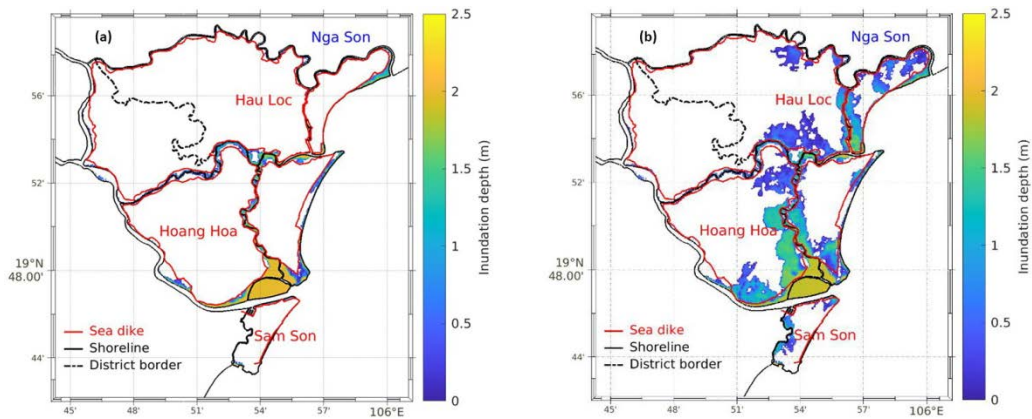


Figure 12. Distribution of maximum inundation depth for simulation scenarios (a) with and (b) without sea dikes along the Thanh Hoa coastline

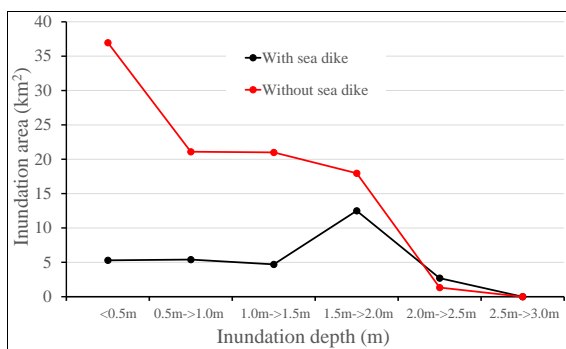


Figure 13. Inundated area by depth range for simulation scenarios (a) with and (b) without sea dikes along the Thanh Hoa coastline

Conclusion

In this study, the numerical model integrating tides, ocean waves, and storm surge (SuWAT) was applied to simulate coastal flooding induced by storm surge combined with tides in the Thanh Hoa coastal zone. The simulation scenarios were conducted by modifying landfall time of Typhoon Doksuri (September 2017), which made landfall during low, mean, and high tidal phases. Additionally, the influence of waves on coastal flooding was assessed by comparing simulations with and without wave effects. A scenario assuming no

sea dikes along the Thanh Hoa coast was also simulated and compared with the case including sea dikes. The main findings of the study are summarized as follows:

(1) For the scenarios of Typhoon Doksuri landfall at the three tidal phases, the largest inundation extent occurs when the typhoon coincides with high tide, followed by mean tide, and the smallest during low tide. The total inundated area in the study region during high-tide landfall is approximately 21.9% larger than in the low-tide scenario.

(2) When wave effects are included, the total inundated area increases by about 7.2% compared with the simulation without waves, and certain areas experience greater inundation depths.

(3) In the scenario without sea dikes, the total inundated area increases by approximately 69.0% compared with the case including dikes. However, in this no-dike scenario, a larger proportion of the flooded area occurs at shallow inundation depths compared with the scenario with sea dikes.

The SuWAT integrated model has been validated in previous studies for flood-inducing factors such as tides, waves, and storm surge during Typhoon Doksuri. Although no observational data are available to directly validate the simulated coastal flooding in Thanh Hoa for Typhoon Doksuri (September 2017), the analysis results above are consistent with the expected roles of tides, waves, and sea dikes in influencing storm-surge-induced coastal flooding. Therefore, the development of flood risk maps based on typhoon scenarios corresponding to different tidal phases is highly valuable for coastal planning, forecasting, and early warning. Moreover, since the highest flooding risk occurs when a typhoon coincides with high tide, areas with elevated flood risk should consider constructing coastal and river dikes to mitigate inundation from storm surges and wave overtopping.

In this study, the effect of river discharge on coastal flooding during typhoons was not considered. Additionally, the flood risk under varying typhoon intensities, in the context of climate change and sea-level rise, remains an

important topic that will be addressed in future research.

Acknowledgments: This research is funded by the Ministry of Science and Technology of Vietnam under grant number ĐTDL-CN-46/22, which the authors gratefully acknowledge.

References

- [1] N. B. Thuy, "Study on the selection of storm surge forecasting models for operational forecasting in Vietnam", *Ministry of Natural Resources and Environment Research Project*, 2017 [in Vietnamese].
- [2] D. D. Chien, N. B. Thuy, N. T. Sao, T. H. Thai, S. Kim, "Study on the interaction between waves and storm surge using a numerical model", *Vietnam Journal of Hydro-meteorology*, 647, 19–24, 2014 [in Vietnamese].
- [3] N. N. Thuy, "Study on the mechanisms of storm surge generation after typhoon landfall along the northern coastal region of Vietnam", *Vietnam Journal of Marine Science and Technology*, 17(4B), 208–216, 2017 [in Vietnamese].
- [4] N. B. Thuy, S. Kim, V. H. Dang, H. D. Cuong, C. Wettre, L. R. Hole, "Assessment of Storm Surge along the coast of Central Vietnam", *J. Coastal Res.*, 33, 518–530, 2017.
- [5] N. B. Thuy, S. Kim, T. N. Anh, N. K. Cuong, P. T. Thuc, L. H. Hole, "The influence of moving speeds, wind speeds, and sea level pressures on after-runner storm surges in the Gulf of Tonkin, Vietnam", *Ocean Eng.*, 212, 107613, 2020.
- [6] P. V. Tien, N. B. Thuy, S. Kim, N. K. Cuong, P. K. Ngoc, M. V. Khiem, L. H. Hole, "Impact of the interaction of surge, wave, and tide on the surge and wave on the northern coast of Vietnam for a marine storm surge and wave forecast system", *Regional Studies in Marine Science*, 87, 2025.
- [7] <https://vtv.vn/trong-nuoc/bao-so-10-gay-mua-lon-tai-thanh-hoa-moi-tuyen-duong-ngap-trong-nuoc-20170915172525371.htm> [accessed August 26, 2025].

- [8] N. T. V. Lien, “Assessment of coastal risk in Thua Thien – Hue Province due to sea-level rise and development of decision support software”, *Independent project – collaboration between the Vietnam Academy of Science and Technology and the People’s Committee of Thua Thien Hue Province*, 2010 [in Vietnamese].
- [9] Vietnam Disaster Management Authority, “Flood risk maps for scenarios of strong and super-typhoons making landfall along the Vietnamese coast”, 2016 [in Vietnamese].
- [10] P. V. Tien, T. T. T. Linh, P. K. Ngoc, B. M. Ha, N. B. Thuy, “Preliminary results on coastal flooding simulation in Thanh Hoa due to storm surge”, *Vietnam Journal of Hydro-Meteorology*, 752, 87–96, 2023 [in Vietnamese].
- [11] S. Lee, T. Kang, D. Sun and J. J. Park, “Enhancing an Analysis Method of Compound Flooding in Coastal Areas by Linking Flow Simulation Models of Coasts and Watershed”, *Sustainability*, Vol. 12/ 6572, 2020.
- [12] S. Dasgupta, M. Huq, Z. H. Khan, M. M. Z. Ahmed, N. Mukherjee, M. Khan, K. D. Pandey, “Vulnerability of Bangladesh to cyclones in a changing climate: Potential damages and adaptation cost”, *World Bank Policy Research Working Paper*, 2010.
- [13] S. Val, G. Sarah, P. Paul, C. Ray, B. Curtis, S. Yuri, “Early Warnings of Coastal Inundation” [Online], WMO, 2019. Available: <https://public.wmo.int/en/resources/bulletin/early-warnings-of-coastal-inundation>. [accessed August 26, 2025].
- [14] K. Yang, V. A. Paramygin, Y. P. Sheng, “A Rapid Forecasting and Mapping System of Storm Surge and Coastal Flooding (2020)”, *Weather and Forecasting*, 2020.
- [15] J. Wolf, “Coastal flooding: impacts of coupled wave–surge–tide models”, *Natural Hazards*, Vol. 49, 241-260, 2008.
- [16] X. Chen, P. Ji, Y. Wu, L. Zhao, “Coupling simulation of overland flooding and underground network drainage in a coastal nuclear power plant”, *Nucl. Eng. Des.*, 325, 129–134, 2017.
- [17] S. Lee, T. Kang, D. Sun, J. J. Park, “Enhancing an Analysis Method of Compound Flooding in Coastal Areas by Linking Flow Simulation Models of Coasts and Watershed”, *Sustainability*, Vol. 12, 6572, 2020.
- [18] H. Li, L. Lin, K. A. Burks-Copes, “Modeling of Coastal Inundation, Storm Surge, and Relative Sea-Level Rise at Naval Station Norfolk, Norfolk, Virginia, U.S.A”, *Journal of Coastal Research*, 29, 18-30, 2013.
- [19] J. Yin, N. Lin, D. Yu, “Coupled modeling of storm surge and coastal inundation: A case study in New York City during Hurricane Sandy”, *Water Resources Research*, 52, 8685-8699, 2016.
- [20] G. Wu, F. Shi, J. T. Kirby, B. Liang, J. Shi, “Modeling Wave Effects on Storm Surge and Coastal Inundation”, *Coastal Engineering*, Vol. 140, 371-382, 2018.
- [21] P. L. N. Murty, A. D. Rao, K. S. Srinivas, E. P. Rama, P. K. Bhaskaran, “Effect of Wave Radiation Stress in Storm Surge-Induced Inundation: A Case Study for the East Coast of India (2020)”, *Pure and Applied Geophysics*, Vol. 177, 2993–3012, 2020.
- [22] S. Y. Kim, H. Mase, K. Kawasaki, M. Tuhi, H. Mizutani, T. Hiraishi, “Surge-wave-tide prediction model including transient wave runup, overtopping and overflow modelling”, *Journal of Japan Society of Civil Engineers Ser B2 (Coastal Engineering)*, 74(2):!_547-!_552, 2018.
- [23] S. Y. Kim, T. Yasuda, H. Mase, “Storm Surge Simulations Occurred in Tosa Bay by Using Surge-Wave-Tide Coupled Model”, *Annual Journal of Coastal Engineering, JSCE*, 55, 321-325, 2008.
- [24] S. Y. Kim, T. Yasuda, H. Mase, “Wave set-up in the storm surge along open coasts during Typhoon Anita”, *Coastal Engineering, ASCE*, (57), 631-642, 2010.
- [25] <https://www.ecmwf.int/en/forecasts/dataset/ecmwf-reanalysis-v5> [accessed August 26, 2025].